

Renormalization of charge due to magnetic monopoles in the Villain form of U(1) lattice gauge theory

H. Kleinert and W. Miller*

Institut für Theorie der Elementarteilchen, Arnimallee 14, 1000 Berlin 33, West Germany

(Received 16 January 1987)

We give an exact equation for the renormalization of the electric charge in the Villain version of the U(1) lattice gauge theory. It involves a sum of monopole loops of increasing size plus their long-range Biot-Savart-type interactions. We count and evaluate the contributions of these loops explicitly up to tenth order. The resulting renormalized charge is in very good agreement with recent Monte Carlo data except in the extreme vicinity of the critical point.

I. INTRODUCTION

The compact U(1) lattice gauge theory is a prototype for understanding quark confinement. For small field fluctuations it describes electromagnetic waves. For large fluctuations, the energy is periodic in the field variables. This gives rise to defects, which have the character of magnetic monopoles with long-range Coulomb interactions.^{1,2} In the three dimensions the magnetic monopoles are pointlike and undergo a magnetic version of Debye screening. This leads to a permanent confinement of electric charges. In four dimensions, the magnetic monopoles form closed world lines to be called monopole loops. As long as the stiffness parameter β of the electromagnetic field fluctuations is high, these loops are small objects with dipole-dipole interactions. They are unable to screen the forces between the magnetic monopoles and there exists no charge confinement.³ If, however, the stiffness parameter β is decreased below a certain critical value, then the configurational entropy of the monopole loops leads to their unlimited growth. The dipole-dipole interaction is taken over by long-range Biot-Savart interactions and the magnetic charges are screened. This is completely analogous to the destruction of Biot-Savart-type long-range forces between vortex loops in superfluid helium if the temperature exceeds a critical value, where the loops grow infinitely large.^{1,4}

As long as the monopole loops are small, it is relatively straightforward to calculate their effect on observable quantities. In this paper we focus our attention on the electric charge e , as a particular example. The reason for this choice is the existence of quite accurate Monte Carlo data on this quantity.⁵⁻⁷ In the absence of monopoles, e^2 is equal to the inverse of the stiffness parameter β . The monopole loops lead to an enhancement of e^2 for decreasing stiffness, which becomes quite dramatic close to the critical point. Still, it is generally believed that the

charge does not diverge near this point. This belief is based on the close similarities of the Migdal-Kadanoff recursion relation for the U(1) lattice gauge theory in four dimensions and the xy model in two dimensions.⁸ In the two-dimensional case the renormalization is due to pointlike monopole vortices. There exists a renormalization-group equation for the electric charge by Kosterlitz and Thouless which makes this problem one of the best understood examples of charge renormalization near a critical point. The charge grows smoothly up to the phase transition point and has no divergence (except for a discontinuous jump to infinity at the transition point itself).

In order to make things as simple as possible, we choose the Villain form of the U(1) lattice gauge theory. This has the advantage that the action is Gaussian for every particular configuration of monopole loops. There are no difficulties from nonlinearities in the electromagnetic field, and the only problem is the correct counting of the loops and the evaluation of their electromagnetic interaction energies. We shall find that the calculated renormalized charges are in very good agreement with the Monte Carlo data, except in the extreme vicinity of the transition point, where a fully fledged renormalization-group procedure is required, which unfortunately is unknown at this time.

This paper is a detailed and improved version of a Letter.⁹ Since our results require the calculation of a great number of graphical terms, we find it useful to record these graphs and our counting procedure.

II. THE VILLAIN FORM OF THE U(1) LATTICE GAUGE THEORY AND THE MAGNETIC MONOPOLES CONTAINED IN IT

The Villain form of the U(1) lattice gauge to be investigated is defined by the partition function

$$Z = \prod_{\mathbf{x}, i} \int_{-\pi}^{\pi} \frac{dA_i(\mathbf{x})}{2\pi} \sum_{\{n_{ij}(\mathbf{x})\}} \exp \left[-\frac{\beta}{2} \sum_{\mathbf{x}, i < j} (\nabla_i A_j - \nabla_j A_i - 2\pi n_{ij})^2 \right], \quad (1)$$

where \mathbf{x} are the N sites of the $D=4$ hypercubic lattice, A_i is the electromagnetic gauge field living on the links (\mathbf{x}, i) of

the lattice, and ∇_i is the lattice derivative across the links defined by

$$\nabla_i A_j = A_j(\mathbf{x}+i) - A_j(\mathbf{x}) . \quad (2)$$

Note that an external integer-valued electric current would enter the action in the form $i \sum_{\mathbf{x}} \Phi_j(\mathbf{x}) A_j$. This shows that

$$e = \sqrt{1/\beta} \quad (3)$$

can be identified with the bare electric charge of the system. The integer numbers n_{ij} on plaquettes (x, i, j) produce a periodic action which allows for the generation of linelike defects—the world lines of magnetic monopoles. If the stiffness parameter is low these proliferate and cause a phase transition. In order to extract this behavior from the partition function, we proceed as follows.

We introduce a set of auxiliary electromagnetic field tensors $F_{ij}(\mathbf{x})$ on plaquettes and rewrite the partition function as

$$Z = \prod_{\mathbf{x}, i < j} \left[\int \frac{dF_{ij}}{\sqrt{2\pi\beta}} \right] \sum_{\{n_{ij}(\mathbf{x})\}} \exp \left[-\frac{1}{2\beta} \sum_{\mathbf{x}, i < j} F_{ij}^2 + i \sum_{\mathbf{x}, i < j} (\nabla_i A_j - \nabla_j A_i - 2\pi n_{ij}) \right] . \quad (4)$$

We then perform the summation over n_{ij} . This restricts the field tensor F_{ij} to integer numbers f_{ij} . Afterwards, we integrate out the $A_i(\mathbf{x})$ fields which enforces

$$\bar{\nabla}_i f_{ij}(\mathbf{x}) = 0 , \quad (5)$$

where $\bar{\nabla}_i$ has the definition $\bar{\nabla}_i f_{ij} \equiv f_{ij}(\mathbf{x}) - f_{ij}(\mathbf{x}-i)$. Condition (5) implies that the integer numbers $f_{ij}(\mathbf{x})$ on plaquettes form closed surfaces. The partition function now becomes

$$Z = \frac{1}{(2\pi\beta)^{3N}} \sum_{\{f_{ij}(\mathbf{x})\}} \delta_{\bar{\nabla}_i f_{ij}, 0} \exp \left[-\frac{1}{2\beta} \sum_{\mathbf{x}, i < j} f_{ij}^2(\mathbf{x}) \right] . \quad (6)$$

The divergence condition (5) is ensured by introducing a dual integer vector potential $\bar{a}_i(\mathbf{x})$ and decomposing

$$f_{ij}(\mathbf{x}) = \epsilon_{ijkl} \bar{\nabla}_j \bar{a}_l(\mathbf{x}-l) , \quad (7)$$

which can uniquely be done in the gauge $\bar{a}_4(\mathbf{x}) = 0$, apart from some boundary conditions. We then transform the summation over the remaining $\bar{a}_i(\mathbf{x})$ ($i = 1, 2, 3$) into integrals using the Poisson identity:

$$\sum_{\bar{a}_i(\mathbf{x})} = \sum_{\{l_i(\mathbf{x})\}} \int d\bar{A}_i(\mathbf{x}) \exp \left[2\pi i \sum_{\mathbf{x}} l_i(\mathbf{x}) \bar{A}_i(\mathbf{x}) \right] , \quad (8)$$

where $l_i(\mathbf{x})$ ($i = 1, 2, 3$) are integer numbers on links, with the following relation to the jump numbers $n_{ij}(\mathbf{x})$:

$$l_i(\mathbf{x}) = \epsilon_{ijkl} \bar{\nabla}_i n_{kl}(\mathbf{x}+i) . \quad (9)$$

This can be derived from Eqs. (4) and (7). Since we use the gauge $\bar{A}_4(\mathbf{x}) = 0$, we can choose l_4 arbitrarily. We do this in the following way:

$$l_4(\mathbf{x}) = -\frac{1}{\bar{\nabla}_4} [\bar{\nabla}_i l_i(\mathbf{x})] .$$

Then $l_i(x)$ ($i = 1, 2, 3$) is extended to a four-vector l_i ($i = 1, \dots, 4$) satisfying

$$\bar{\nabla}_i l_i = 0 , \quad (10)$$

i.e., the integer numbers on links $l_i(\mathbf{x})$ form closed world lines. These are the monopole loops.

Using (8) we can rewrite the partition function (6) as

$$Z = \frac{1}{(2\pi\beta)^N} \prod_{\mathbf{x}, i} \left[\int \frac{d\bar{A}_i(\mathbf{x})}{\sqrt{2\pi\beta}} \right] \delta_{\bar{A}_4, 0} \delta_{\bar{\nabla}_i l_i, 0} \exp \left[-\frac{1}{2\beta} \sum_{\mathbf{x}, i < j} \bar{F}_{ij}^2 + 2\pi i \sum_{\mathbf{x}, i} l_i \bar{A}_i \right] , \quad (11)$$

where

$$\bar{F}_{ij} = \nabla_i \bar{A}_j - \nabla_j \bar{A}_i \quad (12)$$

is the continuous version of $\epsilon_{ijkl} f_{kl}$. It is the *dual magnetoelectric* field tensor, and $\sum_{\mathbf{x}} \bar{A}_i l_i$ is a local coupling of the magnetic type. Therefore, the magnetic charge is

$$e_{\text{mg}} = 2\pi\sqrt{\beta} .$$

It satisfies, multiplied with the electric charge (3), the well-known Dirac relation

$$ee_{mg} = 2\pi$$

Integrating out the dual gauge field \bar{A}_i , the partition function becomes

$$Z = (2\pi\beta)^{-3/2N} \sum_{\{l(\mathbf{x})\}} \delta_{\bar{\nabla}_i, 0} \exp \left[\frac{\beta}{2} 4\pi^2 \sum_{\mathbf{x}, \mathbf{x}'} l(\mathbf{x}) v(\mathbf{x} - \mathbf{x}') l(\mathbf{x}') \right], \quad (13)$$

where

$$v(\mathbf{x}) = \sum_{\mathbf{k}} \exp(i\mathbf{k} \cdot \mathbf{x}) \frac{1}{2 \sum_{i=1}^4 (1 - \cos k_i a)} \equiv \sum_{\mathbf{k}} \exp(i\mathbf{k} \cdot \mathbf{x}) \frac{1}{|K|^2} \quad (14)$$

is the lattice version of the four-dimensional Coulomb potential. The exponent in Eq. (15) contains the Biot-Savart-type magnetoelectric interactions between the monopole world lines.¹⁰

III. CHARGE RENORMALIZATION

In the absence of magnetic monopoles the electric charge e can be obtained from the correlation function of the electromagnetic field tensor F_{ij} :

$$\frac{1}{6} \sum_{\mathbf{x}} \langle F_{ij}(\mathbf{x}) F_{ij}(\mathbf{x}') \rangle |_{\text{no monopoles}} \equiv \beta \equiv \frac{1}{e^2}. \quad (15)$$

For the renormalized charge we use the same definition except that we allow for the presence of magnetic monopoles:

$$\frac{1}{6} \sum_{\mathbf{x}} \langle F_{ij}(\mathbf{x}) F_{ij}(\mathbf{x}') \rangle \equiv \beta_R \equiv \frac{1}{e_R^2}. \quad (16)$$

Formally, such correlation functions can be constructed from Eq. (4) by adding an interaction term with an external source λ_{ij} ,

$$2\pi i \sum_{i < j} F_{ij} \lambda_{ij}(\mathbf{x}), \quad (17)$$

in the exponent and performing the differentiations with respect to λ_{ij} as follows:

$$\langle F_{ij}(\mathbf{x}), F_{ij}(\mathbf{x}') \rangle = -Z^{-1} \frac{\delta}{\delta \lambda_{ij}(\mathbf{x})} \frac{\delta}{\delta \lambda_{ij}(\mathbf{x}')} Z. \quad (18)$$

This procedure makes it easy to calculate the correlations. In Eq. (4), λ_{ij} enters at the same level as $-2\pi n_{ij}$ so that both arrive at the final formula (13) in the same way, via Eq. (9), i.e., all we have to do is to replace $l_i(\mathbf{x})$ by

$$l_i \rightarrow l_i + \epsilon_{ijkl} \bar{\nabla}_j \lambda_{kl}(\mathbf{x} + i). \quad (19)$$

Differentiating (13) twice according to the rule (18) leads to the correlation function

$$\langle F_{ij}(\mathbf{x}), F_{kl}(\mathbf{x}') \rangle = 2\beta (\delta_{ij} \bar{\nabla} \nabla - \nabla_i \bar{\nabla}_j) / \bar{\nabla} \nabla - 8\pi^2 \beta^2 \left\langle l_i(\mathbf{x}) \frac{\delta_{kl} \bar{\nabla} \nabla - \nabla_k \bar{\nabla}_l}{(\bar{\nabla} \nabla)^2} l_j(\mathbf{x}') \right\rangle_{\text{loop}}, \quad (20)$$

where $\langle \rangle_{\text{loop}}$ indicates the expectation taken within the loop sum (13). Contracting ij with kl gives [remember that $(\delta_{ij} \bar{\nabla} \nabla - \nabla_i \bar{\nabla}_j) / \bar{\nabla} \nabla$ is a transverse field and there are three independent components in the four-dimensional space]

$$\frac{1}{6} \sum_{\mathbf{x}} \langle F_{ij}(\mathbf{x}), F_{kl}(\mathbf{x}') \rangle \equiv \frac{1}{e_R^2} = \beta - \frac{4}{3} \pi^2 \beta^2 \sum_{\mathbf{x}} \left\langle l(\mathbf{x}) \frac{1}{\bar{\nabla} \nabla} l(\mathbf{x}') \right\rangle. \quad (21)$$

We can choose $\mathbf{x}' = 0$ because of translation invariance. The operation $(\bar{\nabla} \nabla)^{-1}$ in the Dirac brackets can directly be executed by going into the momentum space where the sum $\sum_{\mathbf{x}} f(\mathbf{x})$ is the same as $\lim_{k \rightarrow 0} f(\mathbf{k})$. Then we observe that due to the vanishing of the total charge $\sum_{\mathbf{x}} l_i(\mathbf{x})$ the correlation function $\langle l_i(\mathbf{k}) l_i(\mathbf{k}) \rangle$ starts out with the series

$$\langle l_i(\mathbf{k}) l_i(\mathbf{k}) \rangle = Ak^2 + Bk^4 + \dots \quad (22)$$

The operation $(\bar{\nabla} \nabla)^{-1}$ amounts to taking the limit

$(1/k^2) \lim_{k \rightarrow 0}$ of this series which only selects the leading term A . Equivalently, we can perform this operation by applying two derivatives with respect to k :

$$\frac{1}{k^2} \lim_{k \rightarrow 0} \langle l_i(\mathbf{k}) l_i(\mathbf{k}) \rangle = \lim_{k \rightarrow 0} \left[\frac{\partial}{\partial k} \right]^2 \langle l_i(k) l_i(k) \rangle. \quad (23)$$

In x space, this operation can be rewritten as

$$-\frac{1}{8} \sum_{\mathbf{x}} |\mathbf{x}|^2 \langle l_i(\mathbf{x}) l_i(\mathbf{0}) \rangle. \quad (24)$$

Hence, we arrive at the *exact* renormalization equation:

$$\frac{1}{e_R^2} \equiv \beta_R = \frac{1}{e^2} \left[1 + \frac{1}{e^2} \frac{\pi^2}{6} \sum_{\mathbf{x}} |\mathbf{x}|^2 \langle l_i(\mathbf{x}) l_i(\mathbf{0}) \rangle \right]. \quad (25)$$

For small renormalization effects, we can expand the denominator on the right-hand side and end up with an approximate version:

$$e_R^2 \approx e^2 - \frac{\pi^2}{6} \sum_{\mathbf{x}} |\mathbf{x}|^2 \langle l_i(\mathbf{x}) l_i(\mathbf{0}) \rangle, \quad (26)$$

which has been given previously by Cardy¹¹ and discussed further by Luck.¹²

IV. GRAPHICAL EVALUATION

The evaluation of our Eq. (25) proceeds via a graphical expansion. First, we consider the partition function (13). There we have to sum up all closed monopole loops on the lattice including their magnetic forces. We shall write this in the following way:

$$Z = \text{const} \times \left(1 + A_1 \square + A_2 \square\square + A_3 \text{graph} + \dots \right), \quad (27)$$

where the constants A_1, A_2, A_3, \dots followed by a graphical symbol denote the number of the corresponding graphs times the appropriate Boltzmann factors of the magnetic field energy:

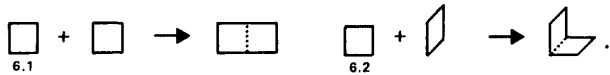
$$\exp \left[-4\pi^2\beta \left(\frac{1}{2} \sum_{\mathbf{x}, \mathbf{x}'} l(\mathbf{x}) v(\mathbf{x} - \mathbf{x}') l(\mathbf{x}') \right) \right].$$

The counting of the graphs proceeds in the following manner.

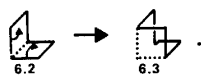
We begin with the smallest graph; this is a graph of length four which will be called the *four-graph*. Larger graphs are developed by composition plus some deformations. There exists only one type of the *four-graph*:



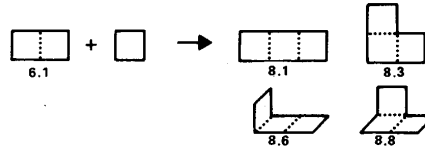
It occupies two dimensions which can be selected in $\binom{D}{2}$ ways out of the D -dimensional space under consideration. Let us ignore, for a moment, this number of arrangements. The six-graphs can be obtained by combining two four-graphs which means adding two plaquettes:



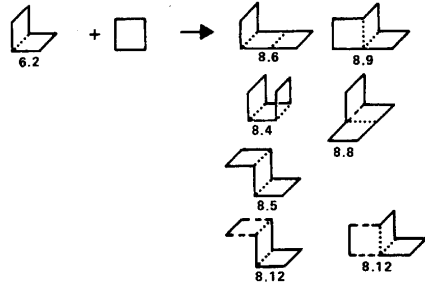
In addition, there exists a three-dimensional six-graph which is not a composition of two plaquettes. Instead, the graph can be constructed by flipping two edges of a three-dimensional one constructed before:



The eight- and ten-graphs require more attention, since their number is considerably larger than that of the six-graphs. Nevertheless, the systematic procedure of counting is quite similar. We take the first six-graph and add a plaquette to the links of the six-graph, such as to form eight-graphs. There exist four possibilities of doing so:



Then we take the second six-graph and do the same. This time there are five three-dimensional eight-graphs and two four-dimensional ones (a plaquette sticking out into the fourth dimension is characterized by dashed border lines):

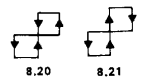


Two of the three-dimensional graphs have already been constructed from the graph 6.1 (namely, 8.6 and 8.8), so only three new ones are left. The two four-dimensional graphs have a different geometry but the same lattice Coulomb potential.

Now we go on in the same way with graph 6.3. Afterwards we have to try turning the edges of each constructed eight-graph and find the missing graphs. For example,



Furthermore, in the case of eight-graphs there exist disconnected graphs, consisting of two four-graphs. For the correct count we have to keep in mind that all graphs carry a magnetic current which gives the Biot-Savart-type electromagnetic interaction. In the case of two separated loops, the direction of the magnetic current in the two separated loops can always be ordered in two different ways. For example,



Therefore, we have two contributions to the summation (25), one with a positive and one with a negative sign of opposite Coulomb interactions between the two loops. It should be noted that the number of disconnected graphs grows with the size of the lattice while the Coulomb interaction decreases for increasing distance of the separated loops. The second effect is stronger than the first so that the sum over two-loop contributions converges rapidly when adding disconnected graphs with larger and larger distances between the disconnected graphs. In our calculations, which we compare to existing Monte Carlo data on finite-size lattices, we have computed all disconnected graphs on a lattice of precisely that size. Up to a distance of four lattice spacings between interacting links we treat the Coulomb potential exactly. At greater distance, it is sufficient to use the asymptotic form $v(r) \approx 1/(4\pi r^2)$.

We can go on with the same procedure used above for the eight-graphs to construct the ten-graphs. In the following we give some examples:

Hence, we arrive at the *exact* renormalization equation:

$$\frac{1}{e_R^2} \equiv \beta_R = \frac{1}{e^2} \left[1 + \frac{1}{e^2} \frac{\pi^2}{6} \sum_{\mathbf{x}} |\mathbf{x}|^2 \langle l_i(\mathbf{x}) l_i(0) \rangle \right]. \quad (25)$$

For small renormalization effects, we can expand the denominator on the right-hand side and end up with an approximate version:

$$e_R^2 \approx e^2 - \frac{\pi^2}{6} \sum_{\mathbf{x}} |\mathbf{x}|^2 \langle l_i(\mathbf{x}) l_i(0) \rangle, \quad (26)$$

which has been given previously by Cardy¹¹ and discussed further by Luck.¹²

IV. GRAPHICAL EVALUATION

The evaluation of our Eq. (25) proceeds via a graphical expansion. First, we consider the partition function (13). There we have to sum up all closed monopole loops on the lattice including their magnetic forces. We shall write this in the following way:

$$Z = \text{const} \times \left(1 + A_1 \square + A_2 \square\square + A_3 \text{graph} + \dots \right), \quad (27)$$

where the constants A_1, A_2, A_3, \dots followed by a graphical symbol denote the number of the corresponding graphs times the appropriate Boltzmann factors of the magnetic field energy:

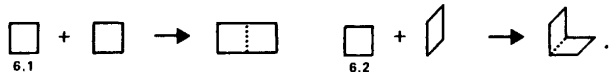
$$\exp \left[-4\pi^2\beta \left(\frac{1}{2} \sum_{\mathbf{x}, \mathbf{x}'} l(\mathbf{x}) v(\mathbf{x} - \mathbf{x}') l(\mathbf{x}') \right) \right].$$

The counting of the graphs proceeds in the following manner.

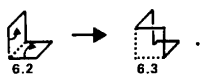
We begin with the smallest graph; this is a graph of length four which will be called the *four-graph*. Larger graphs are developed by composition plus some deformations. There exists only one type of the *four-graph*:



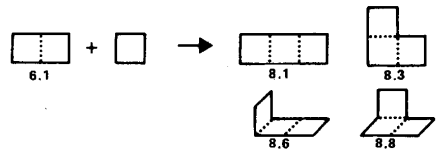
It occupies two dimensions which can be selected in $\binom{D}{2}$ ways out of the D -dimensional space under consideration. Let us ignore, for a moment, this number of arrangements. The six-graphs can be obtained by combining two four-graphs which means adding two plaquettes:



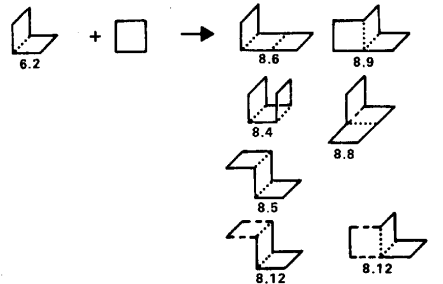
In addition, there exists a three-dimensional six-graph which is not a composition of two plaquettes. Instead, the graph can be constructed by flipping two edges of a three-dimensional one constructed before:



The eight- and ten-graphs require more attention, since their number is considerably larger than that of the six-graphs. Nevertheless, the systematic procedure of counting is quite similar. We take the first six-graph and add a plaquette to the links of the six-graph, such as to form eight-graphs. There exist four possibilities of doing so:



Then we take the second six-graph and do the same. This time there are five three-dimensional eight-graphs and two four-dimensional ones (a plaquette sticking out into the fourth dimension is characterized by dashed border lines):

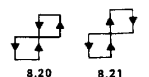


Two of the three-dimensional graphs have already been constructed from the graph 6.1 (namely, 8.6 and 8.8), so only three new ones are left. The two four-dimensional graphs have a different geometry but the same lattice Coulomb potential.

Now we go on in the same way with graph 6.3. Afterwards we have to try turning the edges of each constructed eight-graph and find the missing graphs. For example,

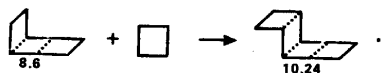


Furthermore, in the case of eight-graphs there exist disconnected graphs, consisting of two four-graphs. For the correct count we have to keep in mind that all graphs carry a magnetic current which gives the Biot-Savart-type electromagnetic interaction. In the case of two separated loops, the direction of the magnetic current in the two separated loops can always be ordered in two different ways. For example,

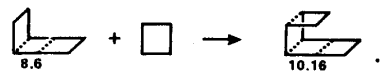


Therefore, we have two contributions to the summation (25), one with a positive and one with a negative sign of opposite Coulomb interactions between the two loops. It should be noted that the number of disconnected graphs grows with the size of the lattice while the Coulomb interaction decreases for increasing distance of the separated loops. The second effect is stronger than the first so that the sum over two-loop contributions converges rapidly when adding disconnected graphs with larger and larger distances between the disconnected graphs. In our calculations, which we compare to existing Monte Carlo data on finite-size lattices, we have computed all disconnected graphs on a lattice of precisely that size. Up to a distance of four lattice spacings between interacting links we treat the Coulomb potential exactly. At greater distance, it is sufficient to use the asymptotic form $v(r) \approx 1/(4\pi r^2)$.

We can go on with the same procedure used above for the eight-graphs to construct the ten-graphs. In the following we give some examples:



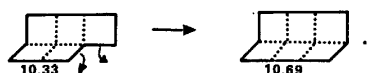
This is a new graph. Another way of adding the plaquette is



But this gives nothing new. This graph has already been obtained earlier, when adding a plaquette to the graph 8.4:

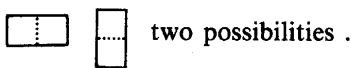


After the construction of all ten-graphs which can be derived from eight-graphs we once again take a look at the possibility of turning the edges in the constructed ten-graphs. For example,



Let us now count the number in which a graph can be arranged in space. This number is obtained by the following procedure: In a D -dimensional space there are $\binom{D}{d}$ possibilities to select a d -dimensional subspace. We have a four-dimensional space and so a plane has $4 \times \frac{3}{2} = 6$ orientations. Because of its cubic symmetry the four-graph has only one possibility in the two-dimensional plane and so the number of the four-graph is $4 \times \frac{3}{2} = 6$.

The graph 6.1 is two dimensional, also, but there exist two directions in which the graph can point:



The total number of graph 6.1 is therefore $2 \times 6 = 12$.

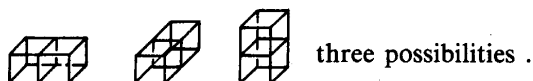
Let us now look at a more complicated graph, e.g., 8.6:



We embed the graph into a rectangle



which is useful for the counting process. First, the graph is three dimensional, and a three-dimensional graph can be arranged in four different ways in the four-dimensional space. Second, the rectangle has three possibilities of orientation in the three-dimensional subspace of the graph:



Third, there exist different arrangements of the graph within the rectangle: (a) the single plaquette can be situated on the right- or left-hand side, $\hat{=}$ two possibilities; (b) the two plaquettes can be situated on four sides, $\hat{=}$ four possibilities. So we get the total number of this type of graph:

$$4 \times 3 \times 2 \times 4 = 96 .$$

The exact count of the four-dimensional graphs is a little bit more cumbersome since one cannot draw a four-dimensional rectangle. We find it easier to use the following procedure: First, we consider the possibilities of a three-dimensional subgraph. In most cases it is given by the construction of the ten-graph via an eight-graph plus a plaquette. Then we count the possibilities to add the four-dimensional part, i.e., a further plaquette. It might be that the multiplicity of the graph is now overestimated since one of the three dimensions can be interchanged with the fourth or that there is a symmetry in the graph, which does not exist in the three-dimensional subgraph. Those graphs have to be identified and omitted. As an example we take the graphs 10.80 and 10.83b. Graph 10.80 consists of the three-dimension graph 8.5, which has 48 possibilities to be arranged in a four-dimensional space, the new plaquette can be added at two sites, always in two directions of the fourth dimension. So the total amount is $48 \times 2 \times 2 = 192$:



There are 96 possibilities for graph 8.6; the new plaquette can be added only at the left-hand side in the two directions of the fourth dimension. This will give the number 192, but because one of the old dimensions can be interchanged with the new one, this number is divided by two, and the total amount is 96:



At this point let us mention that in three dimensions the topologies have been enumerated before, namely, in the 1950s by Wakefield.¹³ In addition, Domb and Sykes¹⁴ developed a special method of counting the total number of graphs without specifying the topologies. Since they do not distinguish between graphs carrying different Coulomb energies, their results are of no use for us. As far as the topology is concerned they quoted the numbers of types for each order up to 10 from Wakefield (for example, three for the six-graphs). Up to order 8, these numbers are in agreement with our calculation. At order 10 there is a difference of four types between Wakefield's and our counting of topologies for the three-dimensional graphs (four less in Wakefield's calculation), whereas our total number of three-dimensional graphs agrees with that of Domb and Sykes. Since we could not find a description of Wakefield's procedure to construct and count his graphs, we had no possibility of detecting where the error might be. The four-dimensional graphs were handled by Fisher and Gaunt¹⁵ who later generalized the method of Domb and Sykes. They also did not specify the topologies of the graphs. Our total number of the four-dimensional eight-graphs agrees with those of Fisher and Gaunt. In the case of four-dimensional ten-graphs, however, we find a total of 432 graphs less than in the paper of Fisher and Gaunt. Fortunately, the

difference is only 1.9% of the total number and thus does not noticeably influence the result of the renormalization.

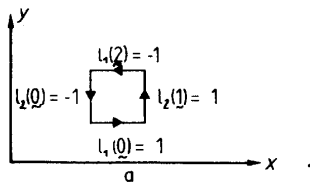
In Table I we have listed the numbers of the different graphs plus their contributions to the energy. The interaction energy of the magnetic current is calculated with the following graphical convention.⁴

We assign the vectors $l_i(\mathbf{x})$ to the links as shown in diagram for the lowest loop diagram, consisting of the vectors

$$l(0) = (1, -1, 0, 0),$$

$$l(1) = (0, 1, 0, 0),$$

$$l(2) = (-1, 0, 0, 0),$$



The total $l_i(\mathbf{x})$ configuration is

$$l_i(\mathbf{x}) = \delta_{x,0} l(0) + \delta_{x,1} l(1) + \delta_{x,2} l(2). \quad (28)$$

The interaction energy is then obtained as follows:

$$\begin{aligned} v_{4,1} &= \frac{1}{2} \sum_{\mathbf{x}, \mathbf{x}'} l(\mathbf{x}) v(\mathbf{x} - \mathbf{x}') l(\mathbf{x}') \\ &= \frac{1}{2} \{ v(0) [l^2(0) + l^2(1) + l^2(2)] + 2v(1) [l(0)l(1) \\ &\quad + l(0)l(2)] + 2v(1,1) l(1)l(2) \} \\ &= 2[v(0) - v(1)]. \end{aligned} \quad (29)$$

One can easily see that only parallel links contribute to the summation, so the pattern of calculation is to consider all parallel links, count their distance x , and to sum up all the Green's function $v(x)$ with these distances. Since each loop is associated with a single plaquette, there are $4 \times \frac{3}{2}$ different loops. (We ignore in Table I the two different orientations of the current.)

Hence, the number A_1 is equal to

$$A_1 = 6 e^{-4\pi^2 \beta v_{4,1}}, \quad (30)$$

where

$$\begin{aligned} v_{4,1} &= \frac{1}{2} \sum_{\mathbf{x}, \mathbf{x}'} l_i(\mathbf{x}) v(\mathbf{x} - \mathbf{x}') l_i(\mathbf{x}') \\ &= 2[v(0) - v(1)] = 0.25 \end{aligned} \quad (31)$$

is the Biot-Savart-type energy of the loop.

For each graph, the data are listed in Table I which has to be read in the following way.

As an example we take the second row of the six-graphs:

$$2. \quad \text{[Diagram of a square loop]} \quad 12(3) \quad 8 \quad (-2, -1, 0, 0, 0, 0, 0, 0, 0, 0, 0, 0, 0, 0, 0, 0).$$

The number 2 is just the running number of six-graphs (graphs of total loop length six). The number 12(3) means

that there are 12 $\binom{D}{3}$ different graphs of this type in D dimensions. The number 3 in the parentheses is the dimension of the graph itself. The number 8 is the sum $-\sum_{\mathbf{x}, \mathbf{x}'} |\mathbf{x} - \mathbf{x}'|^2 l(\mathbf{x}) l(\mathbf{x}')$ which is needed for the evaluation of the charge renormalization and will be discussed below. The row vector lists the interaction potentials between the (parallel) links contributing to this graph.

The entries denote the following lattice potentials:

Green's functions	Code in the table
(1) position: $v(1)$	$=v(1, 0, 0, \dots, 0)$
(2) position: $v(1, 1)$	$=v(0, 1, 0, \dots, 0)$
(3) position: $v(1, 2)$	$=v(0, 0, 1, \dots, 0)$
(4) position: $v(1, 3)$	$=v(0, 0, 0, 1, \dots, 0)$
(5) position: $v(1, 1, 1)$	$=v(0, 0, 0, 0, 1, \dots, 0)$
(6) position: $v(1, 1, 2)$	$=v(0, 0, 0, 0, 0, 1, \dots, 0)$
(7) position: $v(1, 1, 3)$	$=v(0, \dots, 1, 0, 0, 0, 0)$
(8) position: $v(1, 1, 1, 1)$	$=v(0, \dots, 0, 1, 0, 0, 0)$
(9) position: $v(2)$	$=v(0, \dots, 0, 0, 1, 0, 0)$
(10) position: $v(2, 2)$	$=v(0, \dots, 0, 0, 0, 1, 0)$
(11) position: $v(3)$	$=v(0, \dots, 0, 0, 0, 0, 1)$
	$v(1, 1, 1, 2) = v(12)$

The numerical values for these potentials are listed in Table II. In our example, graph 6.2, the vector $(-2, -1, 0, 0, 0, 0, 0, 0, 0, 0, 0, 0, 0, 0, 0, 0)$ implies the interaction potential $-2v(1) - v(1, 1)$. This has to be added to the self-energy of each graph, which for n links is $(n/2)v(0)$. Since this is common to many graphs it is noted only once on the top of the graphs of the same length. Thus, in our example, the total energy is

$$v_{6,2} = 3v(0) - 2v(1) - v(1, 1).$$

The numerical values for these potentials are taken from Table II. This gives a Boltzmann factor for graph 6.2:

$$\begin{aligned} e^{-4\pi^2 \beta v_{6,2}} &= e^{-4\pi^2 \beta [3v(0) - 2v(1) - v(1, 1)]} \\ &= e^{-4\pi^2 \beta \times 0.3922} \end{aligned}$$

Together with the multipliers $12\binom{D}{3}$, which in $D=4$ dimensions is 48, we find the contribution $2 \times 48 e^{-4\pi^2 \beta \times 0.3922}$ to the partition function Z . The factor 2 accounts for the two orientations of the internal magnetic current.

Let us now return to the charge renormalization. According to formula (25) we have to calculate $\sum_{\mathbf{x}} |\mathbf{x}|^2 \langle l(0) l(\mathbf{x}) \rangle$. So we need the correlation of all pairs of two links $l(0)$ and $l(\mathbf{x})$ which are contained in every possible graphs. The loops carry the Boltzmann factor evaluated above for the partition function Z . At the end we have to sum over all the possible positions of $l(\mathbf{x})$. The simplest way to proceed is the following: We take a graph from the expansion of Z (27) and arrange two current elements on the links of the graph in a certain combination, thereby multiplying the original graph of the Z expansion by the factor $|\mathbf{x} - \mathbf{x}'|^2 l(\mathbf{x}) l(\mathbf{x}')$. Then we sum over all \mathbf{x} and \mathbf{x}' .

Systematically, the expansion proceeds as follows:

$$Z \cdot \sum_{\mathbf{x}} |\mathbf{x}|^2 \langle I(\mathbf{0})I(\mathbf{x}) \rangle$$

$$= \tilde{A}_1 \square + \tilde{A}_2 \square\square + \tilde{A}_3 \square\square\square + \dots$$

$$+ A_1 \square \tilde{A}_1 \square + A_1 \square \tilde{A}_2 \square\square + \dots$$

$$+ A_2 \square \tilde{A}_1 \square + A_2 \square\square \tilde{A}_2 \square\square + \dots$$

$$+ \dots$$

$$= Z (\tilde{A}_1 \square + \tilde{A}_2 \square\square + \tilde{A}_3 \square\square\square + \dots),$$

$$\tilde{A}_i = A_i \cdot \sum_{\mathbf{x}, \mathbf{x}'} |\mathbf{x} - \mathbf{x}'|^2 I(\mathbf{x})I(\mathbf{x}').$$

Only the interactions from loop to loop have to be counted since the self-interactions of the loops have already been taken care of in the connected graphs.

The calculation of $\sum_{\mathbf{x}, \mathbf{x}'} |\mathbf{x} - \mathbf{x}'|^2 I(\mathbf{x})I(\mathbf{x}')$ proceeds in complete analogy to that of the Biot-Savart-type energy. From graph 4.1, for example, we obtain

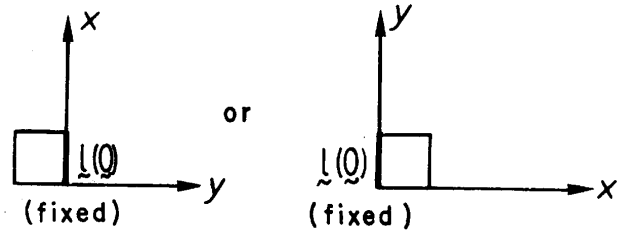
$$\sum_{\mathbf{x}, \mathbf{x}'} |\mathbf{x} - \mathbf{x}'|^2 I(\mathbf{x})I(\mathbf{x}')$$

$$= 2[1^2\{I(\mathbf{0})I(\mathbf{1}) + I(\mathbf{0})I(\mathbf{2})\} + (1^2 + 1^2)I(\mathbf{1})I(\mathbf{2})]$$

$$= -4.$$

The origin of the factor 2 results from the fact that if $I(\mathbf{0})$ is fixed we can put $I(\mathbf{x})$ either on one side or the other in

the dimension under consideration. For example, in the case of graph 4.1,



As mentioned above, for each graph this number can be picked up from the fifth column in Table I. The whole contribution of the graph to the expectation $\sum_{\mathbf{x}} |\mathbf{x}|^2 \langle I(\mathbf{x})I(\mathbf{0}) \rangle$ is given by multiplying the number A_i , evaluated above, and the number $\sum_{\mathbf{x}, \mathbf{x}'} |\mathbf{x} - \mathbf{x}'|^2 I(\mathbf{x})I(\mathbf{x}')$. In our example, graph 6.2, the last one is 8, and

$$A_i = 96 e^{-4\pi^2\beta \times 0.3922}.$$

So we obtain the expectation

$$\tilde{A}_i = -8 \times 96 e^{-4\pi^2\beta \times 0.3922}.$$

Using this procedure, we obtain from (25) the charge renormalization up to loops of length six:

$$\frac{1}{e_R^2} = \frac{1}{e^2} \left\{ 1 - \frac{1}{e^2} \frac{\pi^2}{6} \left[48 \exp \left[-\frac{4\pi^2}{e^2} 0.25 \right] + 384 \exp \left[-\frac{4\pi^2}{e^2} 0.4311 \right] + 768 \exp \left[-\frac{4\pi^2}{e^2} 0.3922 \right] \right. \right.$$

$$\left. \left. + 384 \exp \left[-\frac{4\pi^2}{e^2} 0.4266 \right] \right] \right\}.$$

When continuing this formula up to order 10 using the numbers and energies of Table I, there are so many terms that we refrain from writing them all down. The final result of renormalization is shown in Fig. 1. It is in good agreement with the Monte Carlo data of DeGrand and Toussaint,⁵ also plotted on Fig. 1. When we go into the extreme vicinity of the critical point, our renormalized charge does not increase fast enough. In Fig. 2, our curve is compared with the most recent Monte Carlo simulation of Jersak and co-workers.^{6,7}

We are not able to include the 12-graphs in the counting because of their huge number of different topologies and Coulomb energies.

Clearly, there is the need for a renormalization-group procedure for loops, which is similar to that of Kosterlitz and Thouless for vortex pairs. Only with such a procedure would we be able to approach the vicinity of the critical point.

V. CONCLUSION

We have derived an exact formula for the low-temperature expansion for the renormalization of the

electric charge in the U(1) lattice gauge theory of the Villain form. It is caused by loops of magnetic monopoles. We have calculated this formula up to monopole loops of length ten. Because of the necessity of calculating the Coulomb energies of the various loops and their interactions we could not take over the earlier countings of loop diagrams but had to distinguish carefully the different topologies of graphs. When inserted into our formula the results are in good agreement with Monte Carlo simulations, except very close to the onset of the magnetic Debye screening, where the Coulomb phase collapses and changes into a phase in which electric charges are permanently confined.

ACKNOWLEDGMENT

This work was supported in part by Deutsche Forschungsgemeinschaft under Grant No. K1 256.

TABLE I. The number of graphs, their energy, and their contribution $\sum_{\mathbf{x}, \mathbf{x}'} |\mathbf{x} - \mathbf{x}'|^2 I(\mathbf{x}) I(\mathbf{x}')$ to be extracted as explained in the text.


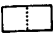



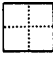
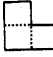

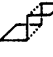


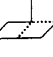
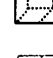
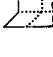
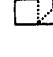
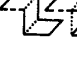

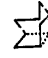


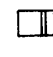
Four-graphs				+ 2v(0)
1.		(2)	4	(-2, 0, 0, 0, 0, 0, 0, 0, 0, 0)
Six-graphs				+ 3v(0)
1.		2(2)	16	(0, -2, 0, 0, 0, 0, 0, 0, -1, 0, 0)
2.		12(3)	8	(-2, -1, 0, 0, 0, 0, 0, 0, 0, 0, 0)
3.		4(3)	12	(0, -3, 0, 0, 0, 0, 0, 0, 0, 0, 0)
Eight-graphs				+ 4v(0)
1.		2(2)	40	(1, -4, -2, 0, 0, 0, 0, 0, 2, 0, -1)
2.		(2)	64	(4, 0, -4, 0, 0, 0, 0, 0, -4, 0, 0)
3.		4(2)	36	(0, 0, -2, 0, 0, 0, 0, 0, -2, 0, 0)
4.		6(3)	4	(-6, 2, 0, 0, 0, 0, 0, 0, 0, 0, 0)
5.		12(3)	20	(-3, 2, -1, 0, -2, 0, 0, 0, 0, 0, 0)
6.		24(3)	20	(-1, -2, -1, 0, 0, 0, 0, 0, 0, 0, 0)
7.		12(3)	32	(2, -2, 0, 0, -2, 0, 0, 0, -2, 0, 0)
8.		48(3)	20	(-1, -1, 0, 0, -1, 0, 0, 0, -1, 0, 0)
9.		24(3)	12	(-1, -4, 0, 0, 1, 0, 0, 0, 0, 0, 0)
10.		12(3)	36	(2, -2, -2, 0, -2, 0, 0, 0, 0, 0, 0)
11.		48(3)	24	(0, -2, -1, 0, -1, 0, 0, 0, 0, 0, 0)
12.		288(4)	6	(-3, 0, 0, 0, -1, 0, 0, 0, 0, 0, 0)
13.		192(4)	8	(-1, -2, 0, 0, -1, 0, 0, 0, 0, 0, 0)
14.		48(4)	10	(0, -2, 0, 0, -2, 0, 0, 0, 0, 0, 0)
15.		96(4)	8	(0, -4, 0, 0, 0, 0, 0, 0, 0, 0, 0)
16.		24(4)	12	(0, 0, 0, 0, -4, 0, 0, 0, 0, 0, 0)
17.		2(2)	0	(-8, 2, 0, 0, 0, 0, 0, 0, 1, 0, 0) + v(0)

TABLE I. (Continued).

18.		(3)	4	$(-6, 1, 0, 0, 0, 0, 0, 0, 0, 0) + v(0)$
19.		(2)	16	$(-8, 0, 0, 0, 0, 0, 0, 0, 0, 0) + 4v(0)$ $+ 2v_{4,1}$
20.		2(2)	8	$(-2, 4, -2, 0, 0, 0, 0, 0, 0, 0)$
21.		2(2)	-8	$(2, -4, 2, 0, 0, 0, 0, 0, 0, 0)$
22.		24(3)	0	$(-1, 2, 0, 0, -1, 0, 0, 0, 0, 0)$
23.		24(3)	0	$(1, -2, 0, 0, 1, 0, 0, 0, 0, 0)$
24.		2(2)	8	$(-1, 0, -2, 0, 0, 0, 0, 0, 4, 0, -1)$
25.		2(2)	-8	$(1, 0, 2, 0, 0, 0, 0, 0, -4, 0, 1)$
26.		12(3)	0	$(-1, -1, 1, 0, 0, 0, 0, 0, 1, 0, 0)$
27.		12(3)	0	$(1, 1, -1, 0, 0, 0, 0, 0, -1, 0, 0)$
28.		3(3)	8	$(4, -4, 0, 0, 0, 0, 0, 0, 0, 0, 0)$
29.		3(3)	-8	$(-4, 4, 0, 0, 0, 0, 0, 0, 0, 0, 0)$
30.		3(3)	8	$(0, 0, -4, 0, 0, 0, 0, 0, 4, 0, 0)$
31.		3(3)	-8	$(0, 0, 4, 0, 0, 0, 0, 0, -4, 0, 0)$
32.		12(3)	8	$(-1, 4, -1, 0, -2, 0, 0, 0, 0, 0, 0)$
33.		12(3)	-8	$(1, 4, -1, 0, 2, 0, 0, 0, 0, 0, 0)$ $+ 5v(0)$
Ten-graphs				
1.		2(2)	72	$(6, 0, -4, -2, 0, 0, 0, 0, -1, -2, -2)$
2.		2(2)	32	$(2, -6, -4, -2, 0, 0, 0, 0, 4, 0, 2) - v(4)$
3.		8(2)	32	$(1, -3, 0, -1, 0, 0, 0, 0, 0, -1, -1)$
4.		4(2)	32	$(1, -1, -1, -1, 0, 0, 0, 0, -2, -1, 0)$
5.		8(2)	50	$(3, 1, -4, -1, 0, 0, 0, 0, -2, -1, -1)$

TABLE I. (Continued).

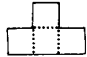
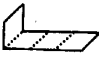




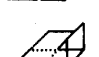

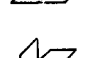
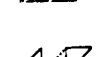

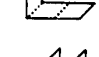
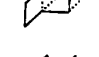
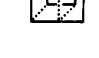
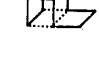
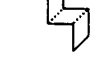






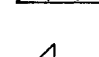
6.		4(2)	38	$(-1, 2, -4, 0, 0, 0, 0, 0, 1, -2, -1)$
7.		24(3)	20	$(0, -4, -2, -1, 0, 0, 0, 2, 0, 0)$
8.		48(3)	20	$(0, -3, 0, 0, -1, -1, 0, 0, 1, 0, -1)$
9.		48(3)	20	$(-1, -1, -2, 0, -2, 0, 0, 0, 2, 0, -1)$
10.		48(3)	34	$(2, 1, -4, 0, 0, -1, 0, 0, -3, 0, 0)$
11.		48(3)	21	$(0, 0, -2, 0, -1, 0, 0, 0, -2, 0, 0)$
12.		48(3)	20	$(-1, -1, -2, 0, 1, -1, 0, 0, -1, 0, 0)$
13.		48(3)	18	$(-1, -1, -1, 0, 0, -1, 0, 0, -1, 0, 0)$
14.		48(3)	20	$(-2, 2, -3, 0, -1, 0, 0, 0, -1, 0, 0)$
15.		24(3)	8	$(-6, 4, 0, 0, -2, 0, 0, 0, -1, 0, 0)$
16.		24(3)	4	$(-4, -3, 0, 0, 2, 0, 0, 0, 0, 0, 0)$
17.		24(3)	8	$(-4, -2, 1, 0, 1, 0, 0, 0, -1, 0, 0)$
18.		24(3)	6	$(-4, -2, 0, 0, 2, 0, 0, 0, -1, 0, 0)$
19.		12(3)	6	$(-6, 2, 0, 0, 0, 0, 0, 0, -1, 0, 0)$
20.		24(3)	16	$(-4, 4, 0, 0, 0, -4, 0, 0, 0, 0, -1, 0)$
21.		48(3)	10	$(-3, -1, 0, 0, 0, -1, 0, 0, 0, 0, 0)$
22.		48(3)	15	$(-2, 0, 0, 0, -1, -1, 0, 0, -1, 0, 0)$
23.		24(3)	16	$(-3, 4, -1, 0, -4, 0, 0, 0, -1, 0, 0)$
24.		24(3)	20	$(-2, 0, 2, -1, -2, -2, 0, 0, 0, 0, 0)$
25.		12(3)	12	$(0, -4, 0, 0, 0, 0, 0, 0, 0, -1, 0)$
26.		48(3)	12	$(0, -5, -3, 0, 1, 1, 0, 0, 1, 0, 0)$
27.		24(3)	16	$(0, -3, 0, 0, 0, -1, 0, 0, -1, 0, 0)$
28.		48(3)	12	$(-1, -3, -1, 0, 0, 0, 0, 0, 0, 0, 0)$

TABLE I. (Continued).


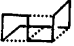


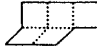
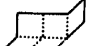
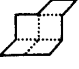
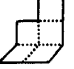
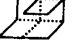

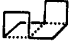









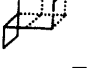
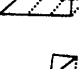

29.		48(3)	13	(-2, 0, -2, 0, -2, 1, 0, 0, 0, 0, 0)
30.		48(3)	10	(-3, 0, 0, 0, -1, 0, 0, 0, -1, 0, 0)
31.		12(3)	8	(-2, -2, 2, 0, 0, 0, 0, 0, -3, 0, 0)
32.		12(3)	16	(-2, -2, 2, 0, 0, -2, 0, 0, 0, -1, 0)
33.		48(3)	26	(2, -2, 0, 0, -3, -1, 0, 0, 0, 0, -1)
34.		48(3)	17	(2, -2, -1, 0, -2, 0, 0, 0, -1, 0, 0)
35.		48(3)	26	(0, 1, -1, 0, -1, -2, 0, 0, -2, 0, 0)
36.		48(3)	30	(2, 0, -3, 0, -1, -1, 0, 0, -2, 0, 0)
37.		24(3)	8	(-2, -1, 1, 0, -1, 0, 0, 0, -1, 0, 0)
38.		24(3)	22	(-2, 1, 0, 0, 0, -3, 0, 0, -1, 0, 0)
39.		24(3)	8	(-1, -4, 1, 0, 0, 0, 0, 0, -1, 0, 0)
40.		48(3)	12	(-1, -2, 0, 0, -1, 0, 0, 0, -1, 0, 0)
41.		24(3)	16	(0, -1, 2, 0, -2, -1, 0, 0, -3, 0, 0)
42.		48(3)	10	(-2, -2, 1, 0, -1, -1, 0, 0, 0, 0, 0)
43.		48(3)	4	(0, -5, 0, 0, -2, 2, 0, 0, 0, 0, 0)
44.		12(3)	12	(-2, -3, -2, 0, 2, 0, 0, 0, 0, 0, 0)
45.		24(3)	29	(0, -1, -3, 0, 0, -2, 0, 0, 0, 0, 0)
46.		24(3)	13	(-2, -1, -2, 0, -1, 0, 0, 0, 1, 0, 0)
47.		24(3)	28	(0, 2, -4, 0, -2, -1, 0, 0, 0, 0, 0)
48.		24(3)	24	(1, -2, 0, -1, -3, -1, 0, 0, 1, 0, 0)
49.		24(3)	24	(2, -3, 0, 0, -2, -1, 0, 0, 0, -1, 0)
50.		48(3)	22	(1, -4, 0, -1, -1, -1, 0, 1, 0, 0, 0)
51.		48(3)	18	(-1, -1, 1, 0, -2, -1, 0, 0, 0, -1, 0)

TABLE I. (Continued).





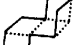
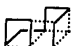

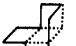
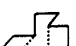

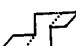


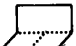
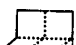
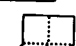
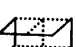
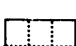
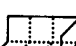


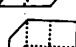
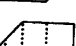
52.		48(3)	8	$(-2, -1, 1, 0, -1, 0, 0, 0, -2, 0, 0)$
53.		48(3)	23	$(1, -2, -2, 0, 0, -1, 0, 0, -1, 0, 0)$
54.		48(3)	8	$(0, -4, 0, 0, -2, 1, 0, 0, 0, 0, 0)$
55.		48(3)	22	$(0, -2, -1, 0, 1, -2, 0, 0, -1, 0, 0)$
56.		48(3)	18	$(-1, -2, -2, 0, 1, -1, 0, 0, 0, 0, 0)$
57.		48(3)	20	$(-1, -4, -1, 0, 0, 0, 0, 0, 1, 0, 0)$
58.		24(3)	22	$(-2, 3, -4, 0, -2, 0, 0, 0, 0, 0, 0)$
59.		48(3)	16	$(-1, 1, -1, 0, -4, 0, 0, 0, 0, 0, 0)$
60.		48(3)	18	$(0, -1, -4, 0, -2, 1, 0, 0, 1, 0, 0)$
61.		24(3)	15	$(0, -3, 0, 0, -1, -1, 0, 0, 0, 0, 0)$
62.		24(3)	16	$(0, -2, 2, -1, -2, -1, 0, 0, 0, 0, 0)$
63.		24(3)	18	$(0, -2, 0, 0, -2, 0, 0, 0, 0, -1, 0)$
64.		24(3)	22	$(0, -3, -2, 0, 2, -2, 0, 0, 0, 0, 0)$
65.		12(3)	40	$(2, 2, -2, 0, 0, -4, 0, 0, -3, 0, 0)$
66.		24(3)	42	$(3, 1, -5, 0, 0, -3, 0, 0, -1, 0, 0)$
67.		24(3)	40	$(4, 0, -4, 0, 0, -2, 0, 0, -3, 0, 0)$
68.		12(3)	8	$(-2, -2, 2, 0, 0, 0, 0, 0, -3, 0, 0)$
69.		12(3)	36	$(4, -3, 0, 0, -4, -2, 0, 0, 2, 0, -2)$
70.		24(3)	36	$(4, -3, 0, -2, -4, -2, 0, 0, 2, 0, 0)$
71.		24(3)	22	$(2, -3, -2, 0, 0, 0, 0, 0, -2, 0, 0)$
72.		24(3)	34	$(2, 1, -4, 0, 0, -2, 0, 0, -2, 0, 0)$
73.		48(3)	46	$(3, 1, -5, 0, 0, -2, 0, 0, -1, 0, 0)$
74.		24(3)	48	$(4, 0, -4, 0, 0, -4, 0, 0, 0, -1, 0)$

TABLE I. (Continued).





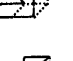
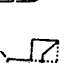
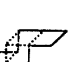




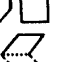
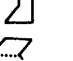
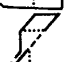
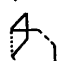
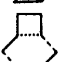
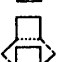


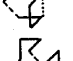



94.		384(4)	20	(1, -2, -1, 0, -2, -1, 0, 0, 0, 0, 0)
95.		384(4)	20	(0, 0, -2, 0, -2, 0, 0, -1, 0, 0, 0)
96.		384(4)	14	(-1, -2, -1, 0, 0, 0, 0, -1, 0, 0, 0)
97.		768(4)	14	(-1, -1, -1, 0, -2, 0, 0, 0, 0, 0, 0)
				
98.		384(4)	14	(0, -3, -1, 0, -1, 0, 0, 0, 0, 0, 0)
99.		768(4)	14	(-1, -2, 0, -1, -1, 0, 0, 0, 0, 0, 0)
				
100.		384(4)	13	(-1, -2, -1, 0, -1, 0, 0, 0, 0, 0, 0)
101.		384(4)	14	(-2, 1, -1, 0, -3, 0, 0, 0, 0, 0, 0)
102.		96(4)	10	(-4, 0, 0, 0, 2, 0, 0, -3, 0, 0, 0)
103.		384(4)	10	(-3, 0, 0, 0, -1, 0, 0, -1, 0, 0, 0)
104.		384(4)	6	(-4, -1, 0, 0, 0, 0, 0, 0, 0, 0, 0)
105.		768(4)	16	(-2, -2, 0, 0, 1, -1, 0, 0, 0, 0, 0) - v(12)
106.		384(4)	10	(-1, -3, 0, 0, -1, 0, 0, 0, 0, 0, 0)
107.		384(4)	10	(-2, 0, 0, 0, -4, 0, 0, 1, 0, 0, 0)
108.		384(4)	10	(-3, 1, 0, 0, -3, 0, 0, 0, 0, 0, 0)
109.		96(4)	10	(-2, -2, 0, 0, 2, -1, 0, -2, 0, 0, 0)
110.		96(4)	6	(-2, -5, 0, 0, 2, 0, 0, 0, 0, 0, 0)
111.		192(4)	16	(0, -3, 0, 0, 0, -1, 0, -1, 0, 0, 0)
112.		384(4)	16	(0, -2, 0, 0, -2, -1, 0, 0, 0, 0, 0)
113.		384(4)	16	(-1, -1, 0, 0, -1, -1, 0, -1, 0, 0, 0)
114.		384(4)	10	(-2, -1, 0, 0, -2, 0, 0, 0, 0, 0, 0)

TABLE I. (Continued).





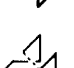


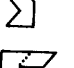

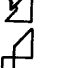

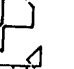
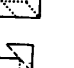

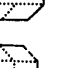


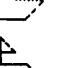


115.		384(4)	16	(0, -2, -1, 0, 0, -1, 0, 0, -1, 0, 0, 0)
116.		384(4)	14	(-1, 1, 0, 0, -5, 0, 0, 0, 0, 0, 0)
117.		384(4)	8	(-4, 1, 0, 0, -2, 0, 0, 0, 0, 0, 0)
118.		192(4)	14	(-1, -2, -1, 0, 0, 0, 0, -1, 0, 0, 0)
119.		192(4)	8	(-3, -2, 0, 0, -1, 0, 0, 1, 0, 0, 0)
120.		192(4)	6	(-3, -3, 0, 0, 1, 0, 0, 0, 0, 0, 0)
121.		192(4)	17	(0, -1, 0, 0, -2, -1, 0, -1, 0, 0, 0)
122.		96(4)	11	(-3, 2, 0, 0, -4, 0, 0, 0, 0, 0, 0)
123.		96(4)	18	(-1, 2, 0, 0, -5, -1, 0, 0, 0, 0, 0)
124.		48(4)	16	(0, -1, -2, 0, 0, 0, 0, -2, 0, 0, 0)
125.		96(4)	20	(2, -3, -2, 0, -2, 0, 0, 0, 0, 0, 0)
126.		768(4)	20	(1, -1, -1, 0, -2, 0, 0, -1, -1, 0, 0)
127.		96(4)	24	(2, 0, 0, 0, -2, 0, 0, -2, -3, 0, 0)
128.		576(4)	16	(1, -3, -1, -2, 0, 0, 0, 0, 0, 0, 0)
129.		384(4)	14	(1, -4, 0, 0, -1, 0, 0, 0, -1, 0, 0)
130.		192(4)	22	(2, -3, 0, 0, -2, -2, 0, 0, 0, 0, 0)
131.		384(4)	23	(1, 0, -1, -3, -1, 0, -1, 0, 0, 0, 0)
132.		192(4)	26	(2, 0, -2, 0, -2, 0, 0, -2, -1, 0, 0)
133.		96(4)	24	(2, 0, -2, 0, -2, 0, 0, -2, -1, 0, 0)
134.		384(4)	22	(1, 0, -2, 0, -3, 0, 0, -1, 0, 0, 0)

TABLE I. (Continued).





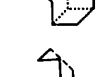
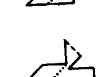









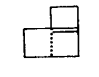


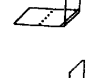
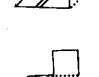
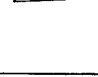


135.		384(4)	18	$(1, -2, 0, 0, -3, -1, 0, 0, 0, 0, 0)$
136.		384(4)	15	$(1, -4, -1, 0, -1, 0, 0, 0, 0, 0, 0)$
137.		96(4)	16	$(0, -3, 0, 0, 0, -1, 0, -1, 0, 0, 0)$
138.		384(4)	24	$(1, 0, 0, 0, -1, -2, 0, -1, 0, 0, 0)$
139.		384(4)	16	$(1, -4, 0, 0, -1, -1, 0, 0, 0, 0, 0)$
140.		384(4)	10	$(0, -4, 0, 0, -2, 0, 0, 1, 0, 0, 0)$
141.		384(4)	12	$(0, -2, 0, 0, -4, 0, 0, 1, 0, 0, 0)$
142.		192(4)	19	$(2, 0, -1, 0, -2, -2, 0, -2, 0, 0, 0)$
143.		96(4)	22	$(0, -1, 0, 0, -2, 0, -2, 0, 0, 0, 0)$
144.		192(4)	8	$(-2, -3, 0, 0, 0, 0, 0, 0, 0, 0, 0)$
145.		96(4)	20	$(0, -1, -2, 0, 0, 0, 0, -2, 0, 0, 0)$
146.		192(4)	22	$(1, 0, -2, 0, -3, 0, 0, -1, 0, 0, 0)$
147.		96(4)	21	$(0, -1, 0, 0, -1, -1, 0, -2, 0, 0, 0)$
148.		96(4)	30	$(2, 0, 0, 0, -2, -3, 0, -3, 0, 0, 0)$
149.		4(2)	16	$(-2, -4, 0, 0, 0, 0, 0, -2, 0, 0) + 3v(0)$
150.		24(3)	8	$(-6, -2, 0, 0, 0, 0, 0, 0, 0, 0) + 3v(0)$
151.		4(2)	2	$(-5, 0, -2, 0, 0, 0, 0, 0, 0, 0) + v(0)$
152.		8(2)	2	$(-4, -4, 2, 0, 0, 0, 0, 0, 0, 0) + v(0)$
153.		12(3)	10	$(-2, -4, 0, 0, 0, 0, 0, 0, 0, 0) + v(0)$
154.		24(3)	5	$(-5, -4, 1, 0, 0, 0, 0, 0, 0, 0) + v(0)$
155.		24(3)	10	$(-3, -2, -1, 0, 0, 0, 0, -2, 0, 0) + v(0)$
156.		24(3)	12	$(-7, 0, 1, 0, 0, 0, 0, 0, 0, 0) + v(0)$
157.		12(3)	8	$(-7, -1, 0, 0, 1, 0, 0, 0, 1, 0, 0) + v(0)$

TABLE I. (Continued).

202.		48(3)	0	$(1, -2, 2, 0, 1, -1, 0, 0, -1, 0, 0)$
203.		48(3)	0	$(-1, 2, -2, 0, -1, 1, 0, 0, 1, 0, 0)$
204.		24(3)	8	$(0, 0, 0, -1, 0, 0, 0, 0, -1, 0, 3) - v(14)$
205.		24(3)	-8	$(0, 0, 0, 1, 0, 0, 0, 0, 1, 0, -3) + v(14)$
206.		48(3)	8	$(0, 0, -1, -3, 0, 0, 0, 0, 1, 0, 3)$
207.		48(3)	-8	$(0, 0, 1, 3, 0, 0, 0, 0, -1, 0, 3)$ $+ 5v(0) + v_{4.1} + v_{6.3}$
208.		48(3)	8	$(-1, 0, 1, -1, 0, -1, 0, 0, 2, 0, 0)$
209.		48(3)	-8	$(1, 0, -1, 1, 0, 1, 0, 0, -2, 0, 0)$
210.		48(3)	8	$(1, 0, 0, 0, -1, -1, 0, 0, 0, 1, 0)$
211.		48(3)	-8	$(-1, 0, 0, 0, 1, 1, 0, 0, 0, -1, 0)$
212.		48(3)	8	$(-2, 2, 2, 0, 0, 0, 0, 0, -2, 0, 0)$
213.		48(3)	-8	$(2, -2, -2, 0, 0, 0, 0, 0, 2, 0, 0)$
214.		48(3)	8	$(1, -1, 1, 0, -2, 1, 0, 0, 0, 0, 0)$
215.		48(3)	-8	$(-1, 1, -1, 0, 2, -, 1, 0, 0, 0, 0, 0)$
216.		48(3)	8	$(-1, 0, 1, -1, 0, -1, 0, 0, 2, 0, 0)$
217.		48(3)	-8	$(1, 0, -1, 1, 0, 1, 0, 0, -2, 0, 0)$
218.		48(3)	8	$(-2, 2, 0, 0, 2, -2, 0, 0, 0, 0, 0)$
219.		48(3)	-8	$(2, -2, 0, 0, -2, 2, 0, 0, 0, 0, 0)$
220.		48(3)	8	$(1, -1, 1, 0, -2, 1, 0, 0, 0, 0, 0)$
221.		48(3)	-8	$(-1, 1, -1, 0, 2, -1, 0, 0, 0, 0, -1)$
222.		48(3)	8	$(0, 0, -2, -2, 0, 0, 0, 0, 2, 0, 2)$
223.		48(3)	-8	$(0, 0, 2, 2, 0, 0, 0, 0, -2, 0, -2)$
224.		48(3)	8	$(0, 0, -1, 1, 0, 0, -1, 0, 0, 0, 2) - v(4)$

TABLE I. (Continued).

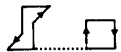
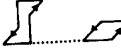
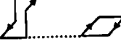

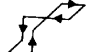


225.		48(3)	-8	$(0,0,1,-1,0,0,1,0,0,0,-2)+v(4)$
226.		48(3)	8	$(0,-1,1,0,0,-1,0,0,0,0,2)-v(4)$
227.		48(3)	-8	$(0,1,-1,0,0,1,0,0,0,0,-2)+v(4)$
228.		48(3)	8	$(-2,2,0,0,2,-2,0,0,0,0,0)$
229.		48(3)	-8	$(2,-2,0,0,-2,2,0,0,0,0,0)$
230.		48(3)	8	$(-1,-1,0,0,1,0,0,0,1,0,0)$
231.		48(3)	-8	$(1,1,0,0,-1,0,0,0,-1,0,0)$

TABLE II. The lattice Coulomb potential in Eq. (16) in four dimensions.

$ x ^2=1(i^2+j^2+k^2+l^2)^{1/2}$	i	j	k	l	$v(x)$
0.0000	0	0	0	0	0.154933
1.0000	0	0	0	1	0.029933
2.0000	0	0	0	2	0.008246
3.0000	0	0	0	3	0.003287
4.0000	0	0	0	4	0.001724
1.4142	0	0	1	1	0.012715
2.2361	0	0	1	2	0.005457
3.1623	0	0	1	3	0.002721
2.8284	0	0	2	2	0.003249
3.6056	0	0	2	3	0.001991
4.2426	0	0	3	3	0.001418
1.7321	0	1	1	1	0.007734
2.4495	0	1	1	2	0.004182
3.3166	0	1	1	3	0.002366
3.0000	0	1	2	2	0.002773
3.7417	0	1	2	3	0.001811
4.3589	0	1	3	3	0.001330
3.3641	0	2	2	2	0.002063
4.1231	0	2	2	3	0.001473
4.6904	0	2	3	3	0.001139
5.1962	0	3	3	3	0.000928
2.0000	1	1	1	1	0.005591
2.6458	1	1	1	2	0.003448
3.4641	1	1	1	3	0.002114
3.1623	1	1	2	2	0.002444
3.8730	1	1	2	3	0.001669
4.4721	1	1	3	3	0.001255
3.6056	1	2	2	2	0.001884
4.2426	1	2	2	3	0.001382
4.7958	1	2	3	3	0.001086
5.2915	1	3	3	3	0.000893
4.0000	2	2	2	2	0.001533
4.5826	2	2	2	3	0.001181
5.0990	2	2	3	3	0.000958
5.5678	2	3	3	3	0.000805
6.0000	3	3	3	3	0.000694

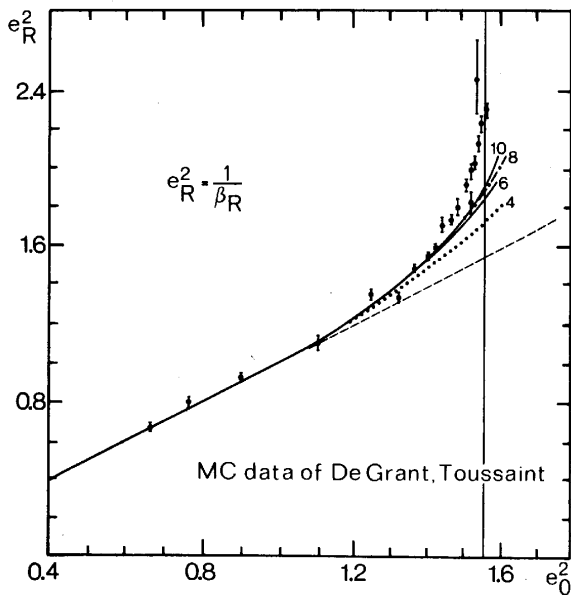


FIG. 1. Renormalized charge e_R as a function of the bare charge e compared with the Monte Carlo data of Ref. 5. The numbers 4, 6, 8, and 10 indicate the sizes of free-monopole loops included in the formula (25).

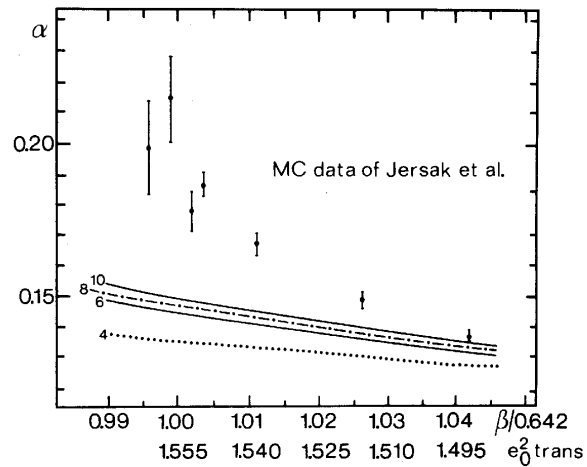


FIG. 2. The renormalized fine-structure constant in the immediate vicinity of the critical point in comparison with the most recent Monte Carlo data of Ref. 6. The curve labels 4, 6, 8, and 10 mean the same as in Fig. 1.

*Present address: Fritz-Haber-Institut der Max-Planck-Gesellschaft, Faradayweg 16, 1000 Berlin 33, West Germany.

¹H. Kleinert, in *Gauge Interactions*, 1982 Les Houches Lectures, edited by G. 't Hooft *et al.* (Plenum, New York, 1984); Phys. Lett. **93A**, 86 (1982).

²T. Banks, R. Meyerson, and J. Kogut, Nucl. Phys. **B129**, 493 (1977).

³A. M. Polyakov, Phys. Lett. **59B**, 82 (1975).

⁴H. Kleinert, *Gauge Theories of Stresses and Defects* (World Scientific, Singapore, 1988).

⁵T. A. DeGrand and D. Toussaint, Phys. Rev. D **24**, 466 (1981).

⁶T. Jersak, T. Neuhaus, and P. M. Zerwas, Phys. Lett. **133B**, 103 (1983).

⁷H. G. Everts, J. Jersak, T. Neuhaus, and P. M. Zerwas, Nucl. Phys. **B251**, 279 (1985).

⁸A. A. Migdal, Zh. Eksp. Teor. Fiz. **69**, 810 (1975) [Sov. Phys. JETP **42**, 413 (1975)]; **69**, 1457 (1975) [**42**, 743 (1975)]; L. P. Kadanoff, Ann. Phys. (N.Y.) **120**, 39 (1979). E. Fradkin and L. Susskind, Phys. Rev. D **17**, 2637 (1978).

⁹H. Kleinert and W. Miller, Phys. Rev. Lett. **56**, 11 (1986).

¹⁰H. Kleinert, in *Gauge Interactions*, proceedings of the International School of Physics "Ettore Majorana," Erice, Italy, 1982, edited by A. Zichichi (Plenum, New York, 1984).

¹¹J. Cardy, Nucl. Phys. **B170**, 369 (1980).

¹²J. M. Luck, Nucl. Phys. **B210**, 111 (1982).

¹³A. J. Wakefield, Proc. Cambridge Philos. Soc. **47**, 419 (1951).

¹⁴C. Domb and M. F. Sykes, Philos. Mag. **2**, 733 (1957); Adv. Phys. **9**, 245 (1960).

¹⁵M. E. Fisher and D. S. Gaunt, Phys. Rev. **133**, A224 (1964).